Biochemical and Biophysical Research Communications 472 (2016) 194–200

Contents lists available at ScienceDirect

Biochemical and Biophysical Research Communications

journal homepage: www.elsevier.com/locate/ybbrc

miR-26b inhibits autophagy by targeting ULK2 in prostate cancer cells

Daguia Zambe John Clotaire [a, b, 1], Bin Zhang [a, 1], Na Wei [a], Rongfang Gao [a], Fei Zhao [a], Yunfei Wang [a], Ming Lei [a, *], Weiwei Huang [a, **]

[a] College of Life Sciences, Northwest A&F University, 3 Taicheng Road, Yangling, Shaanxi Province, 712100, China
[b] Laboratoire des Sciences Agronomiques et Biologiques pour le Développement (LASBAD), Faculty of Science, University of Bangui, Central African Republic

ARTICLE INFO

Article history:
Received 8 February 2016
Accepted 22 February 2016
Available online 23 February 2016

Keywords:
miR-26b
ULK2
Autophagy
Prostate cancer cells

ABSTRACT

Autophagy is a catabolic process widely conserved among eukaryotes that permits the rapid degradation of unwanted proteins and organelles through the lysosomal pathway. The Serine/threonine protein kinase ULK2 (unc-51 like kinase 2) plays an important regulatory role in autophagy thanks to its involvement in mTOR-regulated-initiation and downstream ATG protein-related progression of this catabolic process. An increasing number of miRNAs have been found to modulate autophagy by targeting some ATG genes. In this study, we focus on the role of mir-26b in autophagy in prostate cancer (PCa) cells. We found that miR-26b inhibited autophagy in PC-3 and C4-2 cells, through down-regulation of ULK2 expression. Dual luciferase reporter assays showed that miR-26b binds the 3′UTR of ULK2, suggesting that ULK2 is a direct target of miR-26b. Real-time PCR and Western blot analysis confirmed that over-expression of miR-26b reduced ULK2 mRNA and protein levels. Our results showed also that miR-26b was down-regulated in LNCaP, DU145, C4-2 and PC-3 cells compared to the two normal prostate cells RWPE-1 and WPMY-1 except DU145 cells. This inversely correlates with ULK2 level in the same cell lines. Expression level of ULK2 in tissues microarray (TMA) of prostate cancer derived from 96 patients positively correlated with the pathologic stage of the patients ($*P < 0.05$). Over-expression of ULK2 significantly reversed miR-26b-mediated autophagy inhibition. Taken together, our findings indicate that mir-26b inhibits autophagy through targeting ULK2 which is up-regulated in PCa.

1. Introduction

Autophagy is a cellular degradation pathway in response to stress such as starvation, growth factor deprivation to maintain homeostasis whereby cytoplasmic components including proteins and organelles are engulfed, digested and recycled to sustain cellular metabolism [1,2]. Moreover, autophagy is a pathway used for the elimination of pathogens [3] and engulfment of apoptotic cells [4]. In cancer cells, metabolic stress robustly induces autophagy, which is sustained when apoptosis is blocked [5]. The abnormal regulation of autophagy has been proved to be related with cancer, neurodegenerative and other human diseases. However, the relationship between autophagy and tumor remains controversial [6].

micro-RNAs (miRs), a subclass of regulatory RNAs (18–22 nucleotides), have recently emerged as potential targets for anticancer therapy, as they target about 80% of protein-coding mRNAs and regulate multiple cellular pathways [7]. Through binding the 3′UTR of the target mRNA, miRNA down-regulates its target gene in most cases, and affects cell proliferation [8], apoptosis [9], cell cycle distribution [10] and autophagy [11]. It has been widely reported that deregulated miRNA expression is a common feature of human diseases, especially cancer. Previous studies have demonstrated that several miRNAs are deregulated in prostate cancer tissues or cell lines, and miRNAs deregulation is associated with prostate cancer progression and disease outcome [12,13].

Nowadays, an increasing number of miRNAs, such as miR-17 [14], and miR-372 [11] have been found to modulate autophagy by targeting ATG7 and SQSTM1 respectively in human cancer. miR-

Abbreviations: ULK2, unc-51 like kinase 2; PCa, prostate cancer; miRNAs, microRNAs; $W^{+}mCh^{+}$, wasabi-positive mCherry-positive; $W^{-}mCh^{+}$, wasabi-negative mCherry positive; Rapa, rapamycin; CQ, chloroquine; TMA, tissues microarray.

* Corresponding author.
** Corresponding author.
E-mail addresses: leiming70@hotmail.com (M. Lei), whuang0210@163.com (W. Huang).

[1] These authors contributed equally to this work.

http://dx.doi.org/10.1016/j.bbrc.2016.02.093

26b, a functional miRNA related to tumorgenesis has recently received much attention from researchers [15,16]; its expression is frequently abnormal in tumors, suggesting that it may play a significant role in cancer [17,18]. In our previous computational analysis, ULK2 gene was predicted to be regulated by miR-26b. Like ULK1, ULK2 participates in autophagy regulation. After dephosphorylation at ser1027, ULK2 interacts with Atg13 and FIP200 to activate downstream ATG-related proteins which are essential for many steps in the autophagy pathway [19].

In this study, we investigated the effects of miR-26b in autophagy on PCa cells and demonstrated that ULK2 relied to the autophagy is highly expressed in PCa cells and tissues. Here, we report that ULK2 is down-regulated by miR-26b. miR-26b/ULK2 regulation may have a modulatory effect on autophagy in PCa cells.

2. Materials and methods

2.1. Reagents

LC3B (L7543) antibody, Rapamycin (IPA1021), Chloroquine (C6628-25G), Polybrene (H9268) were from Sigma. ULK2 (sc-10907) antibody and ImmunoCruz goat ABC Staining System (sc-2023) were from Santa Cruz Biotechnology. Goat Anti-Rabbit IgG, Goat Anti-Mouse IgG, Donky Anti-Goat IgG and BCA protein assay kits were from CoWin Biotechnology (Beijing, China). β-actin was from Beyotime Biotechnology (Beijing, China). RNAiso Plus Reagent, cDNA Reverse Transcription Kits, SYBR® PrimeScript™ RT-PCR Kit II, RNAiso for Small RNA, SYBR® PrimeScript™ miRNA RT-PCR Kits and restriction enzymes were from TaKaRa (Dalian, China). Lipofectamine™ LTX with Plus™ Reagent was from Life Technology. Dual-Luciferase Reporter Assay System (E1910) were from Promega (Madison, USA). Puromycin Dihydrochloride (J593) was from Amersco (USA).

2.2. MicroRNAs and DNA plasmid construction

A microRNA mimicking miR-26b-5p and a non-specific microRNA (miR-NC) were from Gene Pharma (Shanghai, China). ULK2 over-expression plasmid (31,966) was purchased from Addgene (USA). The sequences of the wild-type and mutant seed regions of the ULK2 3′UTR were cloned in XhoI-NotI-digested psiCHECK™-2 Vector (Promega). The mutant ULK2 3′UTR sequence was prepared by mutating five (5) nucleotides in the seed region for miR-26b. The sequences of the synthesized oligos were as follows: ULK2 3′UTR-wt forward: 5′-GCCTTTGGGATTACAGCTTGAGT-3′, reverse 5′-TAGTTCCTGACTTTAGGCCAATC-3′; ULK2 3′UTR-mut-site1 forward: 5′-TATGTATTGTATACATAGACCCTTTCCAGA-3′, reverse 5′-AAAATATTTTAAACAAGTCCATTGT-3′; ULK2 3′UTR-mut-site2 forward: 5′-TATGTAATAAACCATTCACCAATTTTAATC-3′, reverse 5′-ATTCAAGCAGGTAAGTAAAAGAAAC-3.

2.3. Cell culture and transfection

Human prostate cancer cell lines LNCaP, DU145, C4-2 and PC-3 were purchased from the China Institute of Basic Medicine, Peking Union Medical. The normal prostate epithelial cell line RWPE-1 and Human prostatic stromal myofibroblast cell line WPMY-1 were purchased from the China center for type culture collection, Wuhan University. LNCaP, DU145, C4-2 and PC-3 cells were cultured in RPMI1640 medium. RWPE-1 cells were cultured in Defined Keratinocyte-SFM (GIBCO, Grand Island, NY, USA). WPMY-1 cells were cultured in DMEM medium. RPMI1640 and DMEM medium were supplemented with 10% fetal bovine serum (Thermo Scientific) and penicillin/streptomycin. Defined Keratinocyte-SFM medium was supplemented only with penicillin/streptomycin. Cells were incubated at 37 °C with 5% CO_2. For transient transfection, Lipofectamine reagent (Life Technologies, Grand Island, NY, USA) was used according to the manufacturer's protocol.

2.4. Quantitative real-time PCR

PC-3 and C4-2 cells were plated in 6-well plates and transfected with 100 pmol of miR-26b for 48 h. Total RNA was isolated using RNAiso Plus Reagent according to the manufacturer's instructions. 500 ng of total RNA was reverse transcribed to cDNA using High-Capacity cDNA Reverse Transcription Kits (RR036A, TaKaRa). Real-time PCR were performed on a Bio-Rad CFX 96 Real-time PCR system using SYBR® PrimeScript™ RT-PCR Kit II (RR820A, TaKaRa) and ULK2-specific primers (forward 5′-GCCAGAAAACTGATTGGGAGGTAGC-3′; reverse 5′-ATCGTGTCTTCACTGAGAGTCCCTT-3′). For miR-26b analysis, reverse transcription and PCR were carried out using a Bulge-Loop ™ miRNA qPCR Primer Set for miR-26b-5p and U6 snRNA (RiboBio, China) according to the manufacturer's instructions. The relative expression levels of ULK2 and miR-26b were respectively normalized to β-actin and U6.

2.5. Luciferase assay

PC-3 and C4-2 cells were plated in 24-well plates and cultured until attachment, then co-transfected with 50 pmol of miR-26b and 50 ng of psiCHECK™-2-ULK2 3′UTR or psiCHECK™-2-ULK2 3′UTR mutant plasmids. Cells were harvested 48 h after transfection, and luciferase activities were analyzed by the Dual-Luciferase Reporter Assay System (Promega, Madison, USA) according to the manufacturer's instructions.

2.6. mCherry-Wasabi fluorescence microscopy

To generate the mCherry-Wasabi-LC3B cell line, supernatant containing lentivirus packaged with mCherry-Wasabi-LC3B was obtained from Genechem Company and added to cultured PC-3 and C4-2 cells. The infection was supplemented with Polybrene at a final concentration of 8 μg/ml. The efficiency of infection was analyzed 48 h later by adding Puromycin for another 48 h. Cells stably expressing mCherry-Wasabi-LC3B were plated in glass-bottomed cell culture dishes at a density of 1×10^5 cells/dish and transfected according to the experiment with miR-26b or ULK2 plasmid together with miR-26b. 48 h post transfection, the cells were washed with PBS three times and examined under a Nikon A1 confocal microscope system (Nikon, Japan). Images were treated with NIS Element Viewer software (Nikon). The average number of LC3B puncta in each cell was calculated to quantify autophagy activity. About 20 cells in each group were used to quantify the LC3B puncta.

2.7. Western blot analysis

Cells were collected after treatment and lysed with lysis buffer (50 mM Tris–HCl pH 7.5, 5 mM EDTA, 0.1% NP-40, 300 mM NaCl, 0.5 mM phenylmethylsulfonyl fluoride and 1 × Roche protease inhibitor cocktail solution). After incubation on ice for 30 min, lysates were cleared by centrifugation at 14,000 g for 15 min at 4 °C and the protein concentrations were determined using BCA protein assay kits CoWin Biotechnology (Beijing, China). Proteins were subjected to SDS-PAGE followed by Western blotting. Protein blots were probed with the indicated primary antibodies and appropriate secondary antibodies and protein bands were visualized using ChemiDoc XRS + imaging system (Bio-Rad, USA).

2.8. Immunohistochemistry (IHC)

The tissues microarray of prostate cancer utilized in this study were obtained from Biomax (#PR1921, US). The slide consists of 80 prostate cancer tissues, 8 prostate adjacent tissues and 8 normal tissues, each sample has a duplicate. IHC is performed by Alena Biotechnology Ltd.Co (Xi'an, China). ULK2 (sc-10907) antibody and ImmunoCruz goat ABC Staining System (sc-2023) were used for IHC staining according to the ABC Staining System protocol. The staining of tissue scores from 0 (negative) to 3 (positive) combining with the intensity of staining and percentage of positive stained cells. Kruskal–Wallis test was used to establish the difference between the groups.

2.9. Statistical analysis

Results are expressed as the mean ± SD. The t-test and u-test were applied to evaluate the differences between groups. For all tests, results were considered significant at $P < 0.05$.

3. Results

3.1. miR-26b inhibits autophagy in PCa cells

In order to investigate the potential involvement of miR-26b in autophagy, we stably transfected PC-3 and C4-2 cells with mCherry-Wasabi-LC3B plasmid using lentivirus. This reporter allows us to distinguish autophagosomes from autophagolysosomes in cells because the pH-sensitive Wasabi fluorophore is inactive in acidic autophagolysosomes. Wasabi-positive mCherry-positive (W^+mCh^+) puncta are autophagosomes and Wasabi-negative mCherry positive (W^-mCh^+) puncta are autophagolysosomes. The stable PC-3 and C4-2 cell line were transfected with miR-26b or control miR-NC for 48 h, then imaged with a confocal microscope. We also used Western blotting to examine the expression of microtubule-associated protein light chain 3 (LC3), which is widely used to monitor autophagy. Fig. 1A and B shows that the number of autophagosomes and autophagolysosomes were lower after miR-26b treatment than miR-NC treatment. To further confirm the inhibition of autophagy by miR-26b, the autophagy flux was analyzed in the presence of Rapamycin; an activator of autophagy and Chloroquine; an inhibitor of autophagy. As shown in Fig.1C, the miR-26b-transfected Rapamycin-treated cells accumulated more LC3-II than the DMSO-treated control cells. More importantly, the LC3-II band was diminished after cells were consecutively transfected with miR-26b and treated with Chloroquine (Fig. 1D). The autophagy flux assay shows that miR-26b can repress the conversion of LC3-I to LC3-II.

Taken together, our data suggest that miR-26b efficiently inhibits autophagy in PC-3 and C4-2 cells.

3.2. miR-26b targets ULK2 in PCa cells

Having shown that miR-26b inhibits autophagy in PC-3 and C4-2 cells, we were interested to find out by which mechanism it operates. We therefore performed miR-26b target prediction in silico using PicTar, miRanda, and Target Scan, and then selected the top candidates from the overlapping results generated by the 3 programs. Among the shortlisted candidates, the autophagy-related gene ULK2 showed two well-conserved miR-26b binding sites with high binding scores in its 3′UTR (starting at positions 656 and 1204); therefore we selected ULK2 for further validation. The alignment of miR-26b with its putative target sequences in the human ULK2 3′-UTR is depicted in Fig.2A.

In order to investigate whether miR-26b could regulate ULK2 in prostate cancer cells as predicted by computational analysis, we constructed a wild-type luciferase reporter vector psiCHECK™2-ULK2 3′-UTR-wt and psiCHECKT^{M2}-ULK2 3′-UTR-mut. Co-transfection experiments showed that miR-26b decreased the luciferase activity of psiCHECK™2-ULK2 3′UTR-wt in PC-3 and C4-

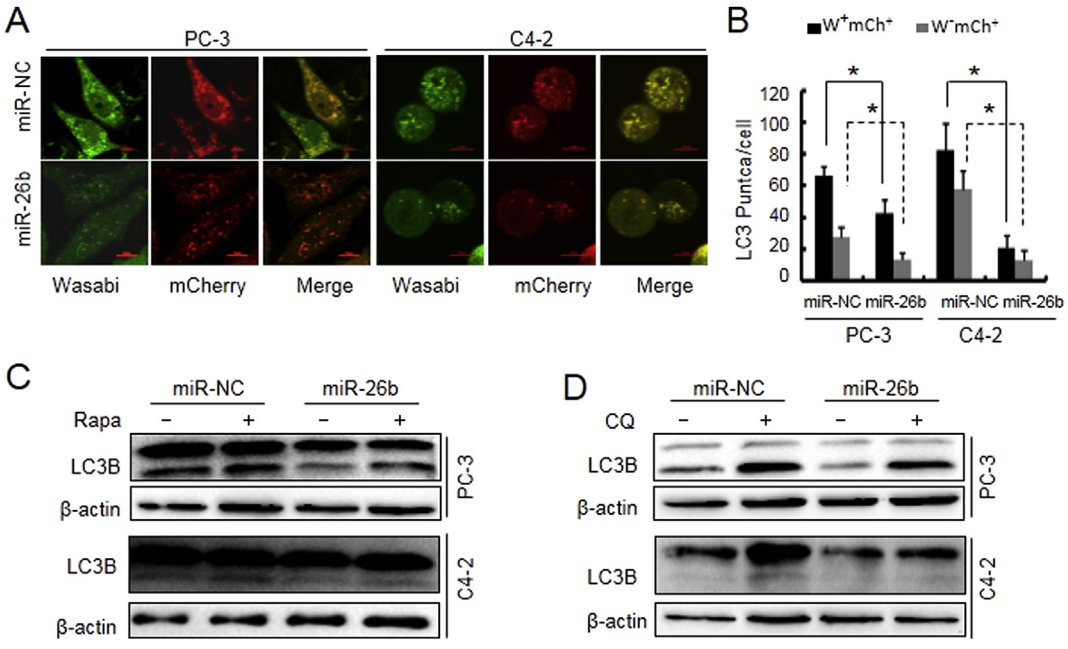

Fig. 1. miR-26b inhibits autophagy in PCa cells. (A, B) PC-3 and C4-2 cells lines stably expressing mCherry-Wasabi-LC3B was transfected with miR-26b or miR-NC and images were acquired with a confocal microscope after 48 h. The graph shows the number of Wasabi-positive mCherry-positive (W^+mCh^+) autophagosomes and Wasabi-negative mCherry positive (W^-mCh^+) autophagolysosomes. Scale bar: 10 μm (C, D) PC-3 and C4-2 cells were transfected with miR-26b or miR-NC for 24 h, and then treated with an autophagy activator (Rapa) or an autophagy inhibitor (CQ) for another 24 h. Cell lysates were then examined for LC3-I and II expression by Western blot. β-actin was used as an internal control.

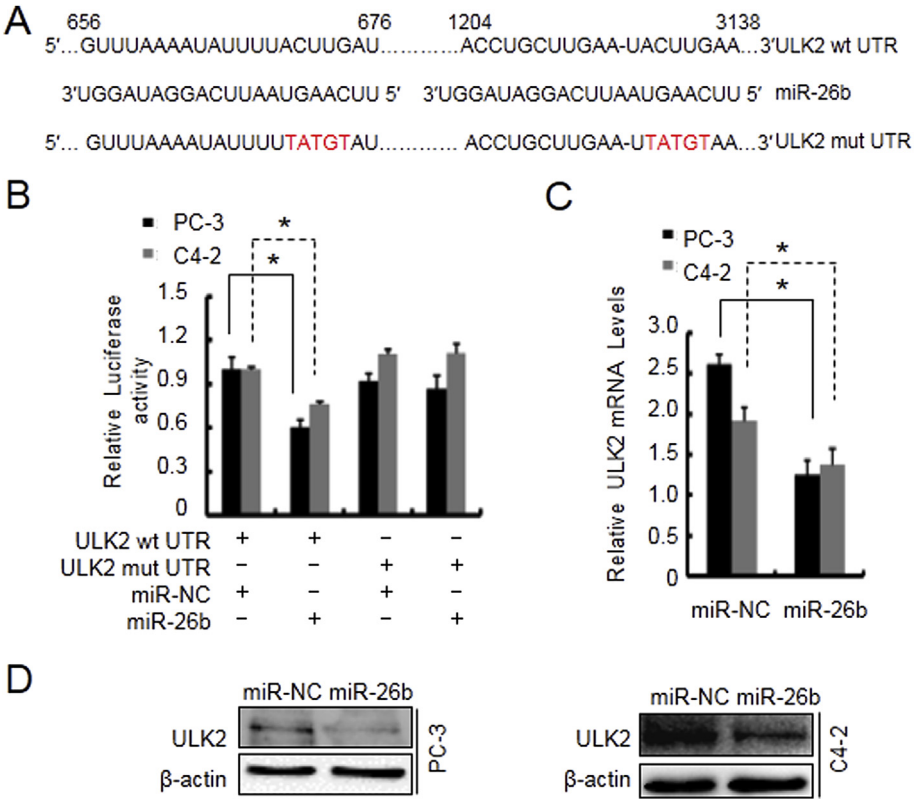

Fig. 2. miR-26b targets ULK2 in PCa cells. (A) Prediction of miR-26b targets was done in silico and ULK2 was selected as one of the top candidates. The bottom line shows the mutations introduced into the two putative miR-26b binding sites. (B) PC-3 and C4-2 cells were transfected with psiCHECK-2 vector containing either the wt ULK2-3′UTR or the mt ULK2-3′ UTR together with miR-26b or miR-NC for 48 h. The activity of Renilla luciferase was normalized to that of firefly luciferase. (C, D) PC-3 and C4-2 cells were transfected with miR-26b or miR-NC for 48 h. Total RNA and lysates were subjected to qRT-PCR and Western blot analysis respectively. β-actin was used as an internal control.

2 cells (Fig. 2B). No reduction was observed in psiCHECK™2-ULK2 3′-UTR-mut, indicating that ULK2 is a direct target of miR-26b.

To further confirm that miR-26b down-regulates ULK2 expression, PC-3 and C4-2 cells were treated with miR-26b or miR-NC for 48 h. Total RNA and cells lysates were obtained and submitted to qRT-PCR and western blot. As shown in Fig. 2C and D, treatment of PC-3 and C4-2 cells with miR-26b significantly decreased the ULK2 mRNA and protein levels as compared to the miR−NC−treated cells.

Taken together, miR-26b down-regulates ULK2 expression in PCa cells.

3.3. Expression level of miR-26b and ULK2 in PCa cells

To address whether the miR-26b-dependent inhibition of autophagy relies on ULK2, we analyzed the expression levels of miR-26b and ULK2 by qRT-PCR. miR-26b was expressed at a lower level in prostate cancer cells LNCaP, DU145, C4-2 and PC-3 compared to two normal prostate cells RWPE-1 and WPMY-1, whereas ULK2 was expressed at a higher level in the same cell lines except DU145. Western blotting showed also that the ULK2 protein level was higher in LNCaP, C4-2 and PC-3 cells than in RWPE-1 and WPMY-1 cells (Fig. 3A). We next performed immunohistochemistry (IHC) analysis on TMA of prostate cancer with specific ULK2 antibodies. As shown in Fig. 3B, the expression level of ULK2 was significantly higher in prostate cancer tissue than in the adjacent normal prostate tissue. miR-26b expression is inversely correlated with ULK2 expression, which suggests that miR-26b may negatively regulate ULK2 in PCa.

3.4. Over-expression of ULK2 rescues miR-26b-mediated autophagy inhibition

Since miR-26b inhibits the expression of ULK2, we decided to investigate whether this inhibition contributes to autophagy regulation in prostate cancer cells. We analyzed the expression levels of the autophagy markers LC3-I and LC3-II after over-expression of ULK2 in PC-3 and C4-2 cells followed by treatment with miR-26b. As shown in Fig. 4A and B, the LC3-I and II protein levels were higher in the ULK2 over-expression cells than in the control. We also cotransfected the stable mCherry-Wasabi-LC3B PC-3 and C4-2 cells with ULK2 and miR-26b or their respective controls. Fig. 4C and D shows that over-expression of ULK2 significantly increases the number of autophagosomes and autophagolysosomes following the treatment with miR-26b. The graph shows the number of Wasabi-positive mCherry-positive (W^+mCh^+) autophagosomes and Wasabi-negative mCherry positive (W^-mCh^+) autophagolysosomes. ULK2 over-expression rescued the decline in autophagy caused by miR-26b; this supports again the hypothesis that miR-26b inhibits autophagy by targeting ULK2.

4. Discussion

miR-26b has recently received much attention from researchers because of its inhibitory effects in cancer cells [20–22]. In this study we evaluated the relationship between miR-26b and autophagy in prostate cancer cells.

Our findings demonstrated that miR-26b down-regulates ULK2 expression and inhibits autophagy in PC-3 and C4-2 cells.

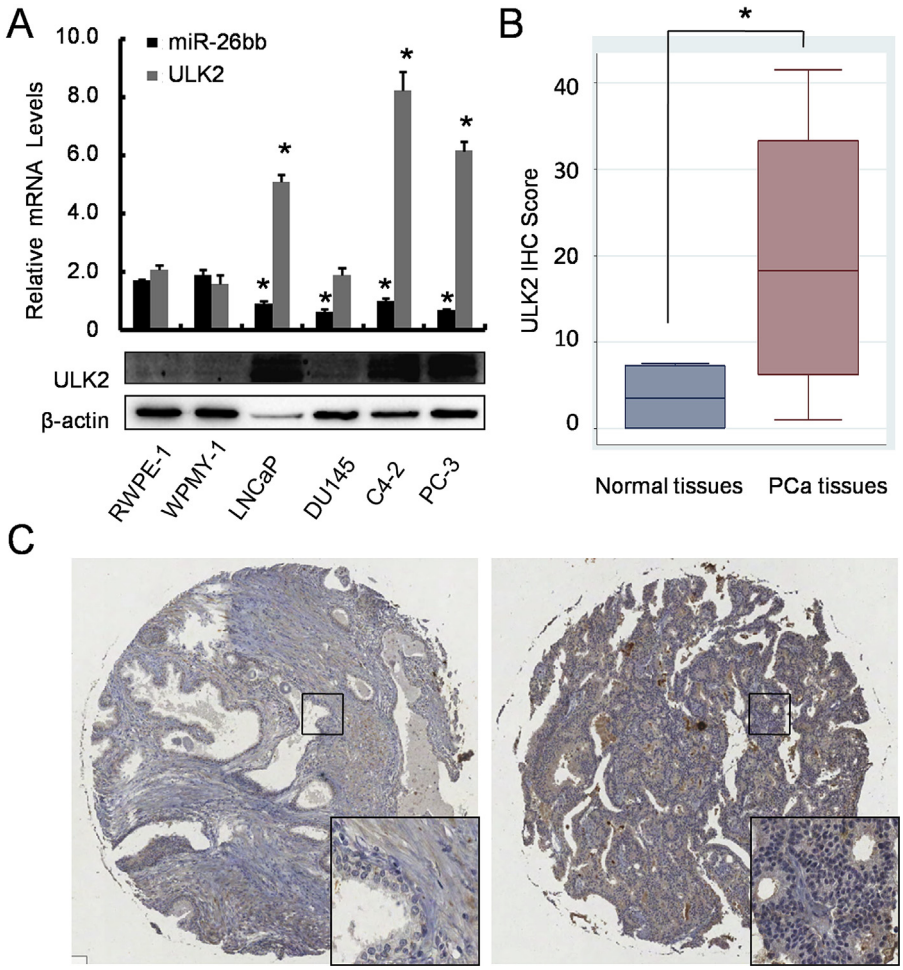

Fig. 3. Expression level of miR-26b and ULK2 in PCa cells and tissues. (A). Total RNA was obtained from RWPE-1, WPMY-1, LNCaP, DU145, C4-2 and PC-3 cells, then miR-26b and ULK2 expression levels were analyzed by RT-qPCR. The graph shows the ULK2 mRNA and miR-26b levels relative to the two normal cells line RWPE-1 and WPMY-1. ULK2 protein level was also analyzed by western blot in the same cells. (B). ULK2 expression level was examined by IHC staining analysis in TMA of prostate cancer derived from 96 patients. (C). A representative example of IHC observed in adjacent normal prostate tissue and prostate cancer tissue using donkey anti-ULK2 antibody were presented. Kruskal–Wallis test was used to evaluate the difference between the groups ($P < 0.05$). β-actin and U6 was used as an internal control.

Furthermore we noticed that the expression level of ULK2 was higher in prostate cancer cells LNCaP, C4-2 and PC-3, than in the normal prostate cells RWPE-1 and WPMY-1. The tissues microarray (TMA) derived from 96 patients showed that ULK2 is significantly over-expressed in prostate tissues as compared to the adjacent normal tissues (Fig. 3B). Conversely, miR-26b was expressed at a lower level in PC-3, C4-2, DU145 and LNCaP cells compared to RWPE-1 and WPMY-1 cells. Consistent with our results, down regulation of miR-26b was also reported in other human cancers, including breast cancer [21,23], lung cancer [24,25], and colorectal cancer [26,27] suggesting a potential role for miR-26b in tumor.

Up-regulation of miR-26b inhibits autophagy, these results were confirmed by Western blot and confocal microscopy analysis of LC3-I and II (Fig. 1). We further confirmed the role of miR-26b in that process by using both activator and inhibitor of autophagy. Rapamycin is known to activate autophagy initiation by targeting mTOR [28]. Treatment of PC-3 and C4-2 cells with miR-26b and the autophagy activator Rapamycin resulted in lower levels of LC3-II, thereby further demonstrating that miR-26b inhibits autophagy (Fig.1C). miR-26b and Chloroquine treatment induced the down-regulation of LC3-II (Fig. 1D). Chloroquine suppresses autophagy flux by blocking fusion of autophagosomes with lysosomes which is considered to be the last step in autophagy degradation [29].

According to Shin Lee et al., ULK2 interacts with Atg13 and FIP200 to activate autophagy [30], however its post-transcriptional regulation remains unclear. We constructed psiCHECK2-ULK2, psiCHECK2-ULK2-mut plasmids and investigate the effect of miR-26b on ULK2. A combination of bioinformatics and dual-luciferase reporter assays identified ULK2 as a direct target of miR-26b (Fig. 2A and B). miR-26b is able to down-regulate ULK2 expression at both mRNA and protein levels in prostate cancer cells PC-3 and C4-2 (Fig. 2C and D). We last up-regulated ULK2 and demonstrated that over-expression of ULK2 significantly rescued miR-26b-mediated autophagy inhibition in PC-3 and C4-2 cells (Fig. 4A, B and 4C). This result again showed the role of ULK2 in the autophagy pathway; it also demonstrated that ULK2 is directly targeted by miR-26b.

In summary, we found that ULK2 is up-regulated in PCa cells and tissues. miR-26b inhibits autophagy in part via down-regulation of ULK2 expression. miR-26b/ULK2 regulation may have a modulatory effect in prostate cancer cells.

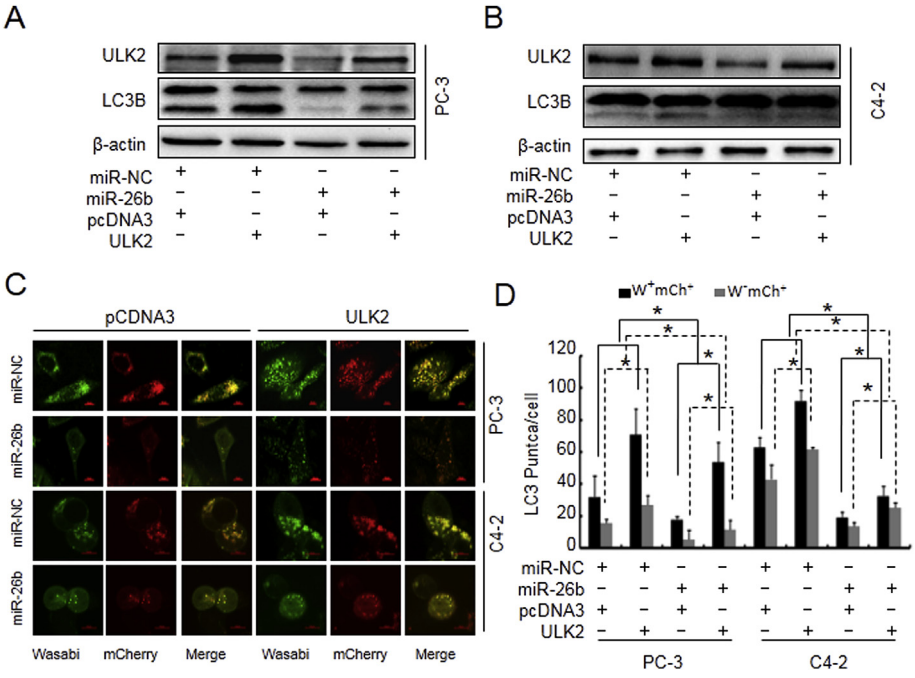

Fig. 4. Over-expression of ULK2 rescues miR-26b-mediated autophagy inhibition (A, B) PC-3 and C4-2 cells were transfected with ULK2 plasmid or control pcDNA3 together with miR-26b or miR-NC for 48 h. Cell lysates were then analyzed by Western blot for LC3-I and II. (C, D) Confocal microscope images of a stable mCherry-Wasabi-LC3B-expressing PC-3 and C4-2 cells line after transfection with ULK2 or control pcDNA3 together with miR-26b or miR-NC. Scale bar: 10 μm β-actin was used as an internal control.

Conflict of interests

M.L and D.Z.J.C conceived the project. D.Z.J.C, B.Z, N.W, R.F.G, Y.F.W and F.Z collected data. D.Z.J.C, B.Z and W.W.H analyzed the data and drafted the manuscript. All authors read and approved the final manuscript and declare no competing financial interests.

Acknowledgments

This work was supported by the National Natural Science Foundation of China (31540002 and 31571194 to Ming Lei; 31300654 to Weiwei Huang), the National instrumentation program (2012YQ030261 to Ming Lei), the Natural Science Foundation of Shannxi Province (2014JQ3098 to Weiwei Huang), the Fundamental Research Funds for the Central Universities (014YB034 to Weiwei Huang) and the Scientific Research Special Fund of National Forestry Public Welfare Project (grant No.201204603 to Ming Lei). Daguia Zambe John Clotaire is supported by the Chinese government and the Central Africa government bilateral cooperation scholarship.

References

[1] B. Levine, D.J. Klionsky, Development by self-digestion: Molecular mechanisms and biological functions of autophagy, Dev. Cell 6 (2004) 463–477.
[2] A.R.J. Young, E.Y.W. Chan, X.W. Hu, R. Koch, S.G. Crawshaw, S. High, D.W. Hailey, J. Lippincott-Schwartz, S.A. Tooze, Starvation and ULK1-dependent cycling of mammalian Atg9 between the TGN and endosomes, J. Cell Sci. 119 (2006) 3888–3900.
[3] M.I. Colombo, Autophagy: A pathogen driven process, IUBMB Life 59 (2007) 238–242.
[4] X.P. Qu, Z.J. Zou, Q.H. Sun, K. Luby-Phelps, P.F. Cheng, R.N. Hogan, C. Gilpin, B. Levine, Autophagy gene-dependent clearance of apoptotic cells during embryonic development, Cell 128 (2007) 931–946.
[5] J.J. Lum, D.E. Bauer, M. Kong, M.H. Harris, C. Li, T. Lindsten, C.B. Thompson, Growth factor regulation of autophagy and cell survival in the absence of apoptosis, Cell 120 (2005) 237–248.
[6] R. Mathew, S. Kongara, B. Beaudoin, C.M. Karp, K. Bray, K. Degenhardt, G.H. Chen, S. Jin, E. White, Autophagy suppresses tumor progression by limiting chromosomal instability, Genes & Dev. 21 (2007).
[7] M. Galasso, S.K. Sandhu, S. Volinia, MicroRNA Expression Signatures in Solid Malignancies, Cancer J. 18 (2012) 238–243.
[8] Y.J. Li, H.X. Wang, K. Tao, Q. Xiao, Z.L. Huang, L. Zhong, W.X. Cao, J.P. Wen, W.L. Feng, miR-29b suppresses CML cell proliferation and induces apoptosis via regulation of BCR/ABL1 protein, Exp. Cell Res. 319 (2013) 1094–1101.
[9] X.Q. He, Y.J. Dong, C.W. Wu, Z.R. Zhao, S.S.M. Ng, F.K.L. Chan, J.I.Y. Sung, J. Yu, MicroRNA-218 Inhibits Cell cycle progression and promotes apoptosis in colon cancer by downregulating BMI1 polycomb ring finger oncogene, Mol. Med. 18 (2012) 1491–1498.
[10] D. Chen, W.J. Guo, Z.P. Qiu, Q.F. Wang, Y. Li, L.H. Liang, L. Liu, S.L. Huang, Y.J. Zhao, X.H. He, MicroRNA-30d-5p inhibits tumour cell proliferation and motility by directly targeting CCNE2 in non-small cell lung cancer, Cancer Lett. 362 (2015) 208–217.
[11] L.F. Feng, Y.N. Ma, J. Sun, Q. Shen, L.M. Liu, H.Q. Lu, F.L. Wang, Y.F. Yue, J.Q. Li, S.J. Zhang, X.Y. Lin, J. Chu, W.D. Han, X. Wang, H.C. Jin, YY1-MIR372-SQSTM1 regulatory axis in autophagy, Autophagy 10 (2014) 1442–1453.
[12] S. Mishra, J.J. Deng, P.S. Gowda, M.K. Rao, C.L. Lin, C.L. Chen, T. Huang, L.Z. Sun, Androgen receptor and microRNA-21 axis downregulates transforming growth factor beta receptor II (TGFBR2) expression in prostate cancer, Oncogene 33 (2014) 4097–4106.
[13] C.Y. Wang, W.Y. Tao, S.B. Ni, Q.Y. Chen, Z.S. Zhao, L. Ma, Y.M. Fu, Z.X. Jiao, Tumor-suppressive microRNA-145 induces growth arrest by targeting SENP1 in human prostate cancer cells, Cancer Sci. 106 (2015) 375–382.
[14] S. Comincini, G. Allavena, S. Palumbo, M. Morini, F. Durando, F. Angeletti, L. Pirtoli, C. Miracco, microRNA-17 regulates the expression of ATG7 and modulates the autophagy process, improving the sensitivity to temozolomide and low-dose ionizing radiation treatments in human glioblastoma cells, Cancer Biol. Ther. 14 (2013) 574–586.
[15] E.T. Verghese, R. Drury, C.A. Green, D.L. Holliday, X.M. Lu, C. Nash, V. Speirs, J.L. Thorne, H.H. Thygesen, A. Zougman, M.A. Hull, A.M. Hanby, T.A. Hughes, MiR-26b is down-regulated in carcinoma-associated fibroblasts from ER-positive breast cancers leading to enhanced cell migration and invasion, J. Pathol. 231 (2013) 388–399.
[16] S. Tan, K.S. Ding, R. Li, W.J. Zhang, G.P. Li, X.J. Kong, P.X. Qian, P.E. Lobie, T. Zhu, Identification of miR-26 as a key mediator of estrogen stimulated cell proliferation by targeting CHD1, GREB1 and KPNA2, Breast Cancer Res. 16 (2014).
[17] N. Wu, X.Z. Zhao, M. Liu, H.Z. Liu, W.C. Yao, Y.Y. Zhang, S.S. Cao, X.K. Lin, Role of MicroRNA-26b in Glioma Development and Its Mediated Regulation on EphA2, Plos One 6 (2011).
[18] J. Cao, T. Guo, Q.S. Dong, J.Q. Zhang, Y.F. Li, miR-26b is downregulated in human tongue squamous cell carcinoma and regulates cell proliferation and metastasis through a COX-2-dependent mechanism, Oncol. Rep. 33 (2015) 974–980.

[19] P.M. Wong, C. Puente, I.G. Ganley, X.J. Jiang, The ULK1 complex Sensing nutrient signals for autophagy activation, Autophagy 9 (2013) 124–137.
[20] Z.C. Zhang, K. Kim, X. Li, M. Moreno, T. Sharp, M.J. Goodheart, S. Safe, A.J. Dupuy, B.A. Amendt, MicroRNA-26b represses colon cancer cell proliferation by inhibiting lymphoid enhancer factor 1 expression, Mol. Cancer Ther. 13 (2014) 1942–1951.
[21] J. Li, X.Y. Li, X.J. Kong, Q.F. Luo, J.F. Zhang, L. Fang, MiRNA-26b inhibits cellular proliferation by targeting CDK8 in breast cancer, Int. J. Clin. Exp. Med. 7 (2014) 558–565.
[22] J.L. Sun, P. Yan, Y.Z. Chen, Y. Chen, J.X. Yang, G.Y. Xu, H.J. Mao, Y. Qiu, MicroRNA-26b inhibits cell proliferation and cytokine secretion in human RASF cells via the Wnt/GSK-3 beta/beta-catenin pathway, Diagn. Pathol. 10 (2015).
[23] D. Anbalagan, G. Yap, Y. Yuan, V.K. Pandey, W.H. Lau, S. Arora, P. Bist, J.S.B. Wong, G. Sethi, P.M. Nissom, P.E. Lobie, L.H.K. Lim, Annexin-A1 regulates MicroRNA-26b*and MicroRNA-562 to directly target NF-kappa B and angiogenesis in breast cancer cells, Plos One 9 (2014).
[24] X. Zhang, D.K. Xiao, Z.Y. Wang, Y.X. Zou, L.Y. Huang, W.X. Lin, Q.H. Deng, H. Pan, J.F. Zhou, C. Liang, J.X. He, MicroRNA-26a/b regulate DNA replication licensing, tumorigenesis, and prognosis by targeting CDC6 in lung cancer, Mol. Cancer Res. 12 (2014) 1535–1546.
[25] H. Arora, R. Qureshi, A.K. Park, W.Y. Park, Coordinated regulation of ATF2 by miR-26b in gamma-irradiated lung cancer cells, Plos One 6 (2011).
[26] C.P. Zhang, J.L. Tong, G. Huang, Nicotinamide phosphoribosyl transferase (nampt) is a target of MicroRNA-26b in colorectal cancer cells, Plos One 8 (2013).
[27] Y.L. Ma, P. Zhang, F. Wang, M.P. Moyer, J.J. Yang, Z.H. Liu, J.Y. Peng, H.Q. Chen, Y.K. Zhou, W.J. Liu, H.L. Qin, Human embryonic stem cells and metastatic colorectal cancer cells shared the common endogenous human microRNA-26b, J. Cell. Mol. Med. 15 (2011) 1941–1954.
[28] S.X. Wang, M.J. Livingston, Y.C. Su, Z. Dong, Reciprocal regulation of cilia and autophagy via the MTOR and proteasome pathways, Autophagy 11 (2015) 607–616.
[29] D.G. McEwan, D. Popovic, A. Gubas, S. Terawaki, H. Suzuki, D. Stadel, F.P. Coxon, D.M. de Stegmann, S. Bhogaraju, K. Maddi, A. Kirchof, E. Gatti, M.H. Helfrich, S. Wakatsuki, C. Behrends, P. Pierre, I. Dikic, PLEKHM1 regulates autophagosome-lysosome fusion through HOPS Complex and LC3/GABARAP proteins, Mol. Cell 57 (2015) 39–54.
[30] S.H. Shin, E.J. Lee, J. Chun, S. Hyun, S.S. Kang, ULK2 Ser 1027 phosphorylation by PKA regulates its nuclear localization occurring through karyopherin beta 2 recognition of a PY-NLS motif, Plos One 10 (2015).